

**A measurement of the total cross section for $e^+e^- \rightarrow$ hadrons at
 $\sqrt{s}=10.52$ GeV**

Abstract

Using the CLEO detector at the Cornell Electron Storage Ring, we have made a measurement of $R \equiv \frac{\sigma(e^+e^- \rightarrow \text{hadrons})}{\sigma(e^+e^- \rightarrow \mu^+\mu^-)} = 3.56 \pm 0.01 \pm 0.07$ at $\sqrt{s}=10.52$ GeV. This implies a value for the strong coupling constant of $\alpha_s(10.52 \text{ GeV}) = 0.20 \pm 0.01 \pm 0.06$, or $\alpha_s(M_Z) = 0.13 \pm 0.005 \pm 0.03$.

Submitted to Physical Review D

12.38.Aw, 12.38.Qk, 13.60.Hb, 13.85.Lg

arXiv:hep-ex/9707018v1 8 Jul 1997

R. Ammar,¹ P. Baringer,¹ A. Bean,¹ D. Besson,¹ D. Coppage,¹ C. Darling,¹ R. Davis,¹
 N. Hancock,¹ S. Kotov,¹ I. Kravchenko,¹ N. Kwak,¹ S. Anderson,² Y. Kubota,²
 M. Lattery,² S. J. Lee,² J. J. O'Neill,² S. Patton,² R. Poling,² T. Riehle,² V. Savinov,²
 A. Smith,² M. S. Alam,³ S. B. Athar,³ Z. Ling,³ A. H. Mahmood,³ H. Severini,³ S. Timm,³
 F. Wappler,³ A. Anastassov,⁴ S. Blinov,^{4,1} J. E. Duboscq,⁴ K. D. Fisher,⁴ D. Fujino,^{4,2}
 K. K. Gan,⁴ T. Hart,⁴ K. Honscheid,⁴ H. Kagan,⁴ R. Kass,⁴ J. Lee,⁴ M. B. Spencer,⁴
 M. Sung,⁴ A. Undrus,^{4,1} R. Wanke,⁴ A. Wolf,⁴ M. M. Zoeller,⁴ B. Nemati,⁵ S. J. Richichi,⁵
 W. R. Ross,⁵ P. Skubic,⁵ M. Wood,⁵ M. Bishai,⁶ J. Fast,⁶ E. Gerndt,⁶ J. W. Hinson,⁶
 N. Menon,⁶ D. H. Miller,⁶ E. I. Shibata,⁶ I. P. J. Shipsey,⁶ M. Yurko,⁶ L. Gibbons,⁷
 S. Glenn,⁷ S. D. Johnson,⁷ Y. Kwon,⁷ S. Roberts,⁷ E. H. Thorndike,⁷ C. P. Jessop,⁸
 K. Lingel,⁸ H. Marsiske,⁸ M. L. Perl,⁸ D. Ugolini,⁸ R. Wang,⁸ X. Zhou,⁸ T. E. Coan,⁹
 V. Fadeyev,⁹ I. Korolkov,⁹ Y. Maravin,⁹ I. Narsky,⁹ V. Shelkov,⁹ J. Staeck,⁹
 R. Stroynowski,⁹ I. Volobouev,⁹ J. Ye,⁹ M. Artuso,¹⁰ A. Efimov,¹⁰ F. Frasconi,¹⁰ M. Gao,¹⁰
 M. Goldberg,¹⁰ D. He,¹⁰ S. Kopp,¹⁰ G. C. Moneti,¹⁰ R. Mountain,¹⁰ S. Schuh,¹⁰
 T. Skwarnicki,¹⁰ S. Stone,¹⁰ G. Viehhauser,¹⁰ X. Xing,¹⁰ J. Bartelt,¹¹ S. E. Csorna,¹¹
 V. Jain,¹¹ S. Marka,¹¹ R. Godang,¹² K. Kinoshita,¹² I. C. Lai,¹² P. Pomianowski,¹²
 S. Schrenk,¹² G. Bonvicini,¹³ D. Cinabro,¹³ R. Greene,¹³ L. P. Perera,¹³ G. J. Zhou,¹³
 B. Barish,¹⁴ M. Chadha,¹⁴ S. Chan,¹⁴ G. Eigen,¹⁴ J. S. Miller,¹⁴ C. O'Grady,¹⁴
 M. Schmidtler,¹⁴ J. Urheim,¹⁴ A. J. Weinstein,¹⁴ F. Würthwein,¹⁴ D. M. Asner,¹⁵
 D. W. Bliss,¹⁵ W. S. Brower,¹⁵ G. Masek,¹⁵ H. P. Paar,¹⁵ S. Prell,¹⁵ M. Sivertz,¹⁵
 V. Sharma,¹⁵ J. Gronberg,¹⁶ T. S. Hill,¹⁶ R. Kutschke,¹⁶ D. J. Lange,¹⁶ S. Menary,¹⁶
 R. J. Morrison,¹⁶ H. N. Nelson,¹⁶ T. K. Nelson,¹⁶ C. Qiao,¹⁶ J. D. Richman,¹⁶ D. Roberts,¹⁶
 A. Ryd,¹⁶ M. S. Witherell,¹⁶ R. Balest,¹⁷ B. H. Behrens,¹⁷ K. Cho,¹⁷ W. T. Ford,¹⁷
 H. Park,¹⁷ P. Rankin,¹⁷ J. Roy,¹⁷ J. G. Smith,¹⁷ J. P. Alexander,¹⁸ C. Bebek,¹⁸
 B. E. Berger,¹⁸ K. Berkelman,¹⁸ K. Bloom,¹⁸ D. G. Cassel,¹⁸ H. A. Cho,¹⁸ D. M. Coffman,¹⁸
 D. S. Crowcroft,¹⁸ M. Dickson,¹⁸ P. S. Drell,¹⁸ K. M. Ecklund,¹⁸ R. Ehrlich,¹⁸ R. Elia,¹⁸
 A. D. Foland,¹⁸ P. Gaidarev,¹⁸ R. S. Galik,¹⁸ B. Gittelman,¹⁸ S. W. Gray,¹⁸ D. L. Hartill,¹⁸
 B. K. Heltsley,¹⁸ P. I. Hopman,¹⁸ J. Kandaswamy,¹⁸ P. C. Kim,¹⁸ D. L. Kreinick,¹⁸
 T. Lee,¹⁸ Y. Liu,¹⁸ G. S. Ludwig,¹⁸ J. Masui,¹⁸ J. Mevissen,¹⁸ N. B. Mistry,¹⁸ C. R. Ng,¹⁸
 E. Nordberg,¹⁸ M. Ogg,^{18,3} J. R. Patterson,¹⁸ D. Peterson,¹⁸ D. Riley,¹⁸ A. Soffer,¹⁸
 B. Valant-Spaight,¹⁸ C. Ward,¹⁸ M. Athanas,¹⁹ P. Avery,¹⁹ C. D. Jones,¹⁹ M. Lohner,¹⁹
 C. Prescott,¹⁹ J. Yelton,¹⁹ J. Zheng,¹⁹ G. Brandenburg,²⁰ R. A. Briere,²⁰ Y. S. Gao,²⁰
 D. Y.-J. Kim,²⁰ R. Wilson,²⁰ H. Yamamoto,²⁰ T. E. Browder,²¹ F. Li,²¹ Y. Li,²¹
 J. L. Rodriguez,²¹ T. Bergfeld,²² B. I. Eisenstein,²² J. Ernst,²² G. E. Gladding,²²
 G. D. Gollin,²² R. M. Hans,²² E. Johnson,²² I. Karliner,²² M. A. Marsh,²² M. Palmer,²²
 M. Selen,²² J. J. Thaler,²² K. W. Edwards,²³ A. Bellerive,²⁴ R. Janicek,²⁴
 D. B. MacFarlane,²⁴ K. W. McLean,²⁴ P. M. Patel,²⁴ and A. J. Sadoff²⁵

¹Permanent address: BINP, RU-630090 Novosibirsk, Russia.

²Permanent address: Lawrence Livermore National Laboratory, Livermore, CA 94551.

³Permanent address: University of Texas, Austin TX 78712

- ¹University of Kansas, Lawrence, Kansas 66045
- ²University of Minnesota, Minneapolis, Minnesota 55455
- ³State University of New York at Albany, Albany, New York 12222
- ⁴Ohio State University, Columbus, Ohio 43210
- ⁵University of Oklahoma, Norman, Oklahoma 73019
- ⁶Purdue University, West Lafayette, Indiana 47907
- ⁷University of Rochester, Rochester, New York 14627
- ⁸Stanford Linear Accelerator Center, Stanford University, Stanford, California 94309
- ⁹Southern Methodist University, Dallas, Texas 75275
- ¹⁰Syracuse University, Syracuse, New York 13244
- ¹¹Vanderbilt University, Nashville, Tennessee 37235
- ¹²Virginia Polytechnic Institute and State University, Blacksburg, Virginia 24061
- ¹³Wayne State University, Detroit, Michigan 48202
- ¹⁴California Institute of Technology, Pasadena, California 91125
- ¹⁵University of California, San Diego, La Jolla, California 92093
- ¹⁶University of California, Santa Barbara, California 93106
- ¹⁷University of Colorado, Boulder, Colorado 80309-0390
- ¹⁸Cornell University, Ithaca, New York 14853
- ¹⁹University of Florida, Gainesville, Florida 32611
- ²⁰Harvard University, Cambridge, Massachusetts 02138
- ²¹University of Hawaii at Manoa, Honolulu, Hawaii 96822
- ²²University of Illinois, Champaign-Urbana, Illinois 61801
- ²³Carleton University, Ottawa, Ontario, Canada K1S 5B6
and the Institute of Particle Physics, Canada
- ²⁴McGill University, Montréal, Québec, Canada H3A 2T8
and the Institute of Particle Physics, Canada
- ²⁵Ithaca College, Ithaca, New York 14850

I. INTRODUCTION

The measurement of the hadronic production cross section in e^+e^- annihilation is perhaps the most fundamental experimentally accessible quantity in quantum chromodynamics (QCD) due to its insensitivity to the fragmentation process. The measured hadronic cross-section is generally expressed in terms of its ratio R to the point cross-section for $\mu^+\mu^-$ production. In QCD, R is directly proportional to the number of colors, depends on quark charges, and varies with energy, both discretely as quark mass thresholds are crossed, and gradually as the strong coupling constant α_s “runs”. So, historically, R measurements have been valuable in verifying quark thresholds, charges, color-counting, and the existence of the gluon.

The theoretical prediction for R is

$$R = R_{(0)}(1 + \alpha_s/\pi + C_2(\alpha_s/\pi)^2 + C_3(\alpha_s/\pi)^3). \quad (1)$$

A calculation appropriate at LEP energies obtained $C_2 = 1.411$ and $C_3 = -12.68$ [1] for five active flavors, in the limit of massless quarks. A recent calculation, applicable to the Υ mass region (four active flavors), has included corrections due to the effects of quark masses and QED radiation to obtain $C_2=1.5245$ and $C_3=-11.52$ at $\sqrt{s}=10$ GeV [2]. The effect of including these additional corrections is a difference of approximately 0.3% in the prediction for R at this energy. $R_{(0)}$ is the lowest-order prediction for this ratio, given by $R_{(0)} = N_c \sum_i q_i^2$, where N_c is the number of quark colors; the sum runs over the kinematically allowed quark flavors. Just below the $\Upsilon(4S)$ resonance, where $b\bar{b}$ production is kinematically forbidden, the lowest-order prediction is therefore obtained by summing over $udcs$ quarks, yielding $R_{(0)}=10/3$. An experimental measurement of R can therefore be used to deduce a value for α_s . In this Article we present a measurement of R using the CLEO detector operating at the Cornell Electron Storage Ring (CESR) at a center-of-mass energy $\sqrt{s}=10.52$ GeV.

II. APPARATUS AND EVENT SELECTION

The CLEO II detector is a general purpose solenoidal magnet spectrometer and calorimeter [4]. The detector was designed to trigger efficiently on two-photon, tau-pair, and hadronic events. As a result, although hadronic event reconstruction efficiencies are high, lower-multiplicity non-hadronic backgrounds require careful consideration in this analysis. Good background rejection is afforded by the high precision electromagnetic calorimetry and excellent charged particle tracking capabilities. Charged particle momenta are measured with three nested coaxial drift chambers with 6, 10, and 51 layers, respectively. These chambers fill the volume from $r=3$ cm to $r=100$ cm, where r is the radial coordinate relative to the beam (z) axis, and have good efficiency for charged particle tracking for polar angles $|\cos\theta| < 0.94$, with θ measured relative to the positron beam direction ($+\hat{z}$). This system achieves a momentum resolution of $(\delta p/p)^2 = (0.0015p)^2 + (0.005)^2$, where p is momentum in GeV/c. Pulse height measurements in the main drift chamber provide specific ionization resolution of 6.5% for Bhabha events, giving good K/π separation for tracks with momenta up to 700 MeV/c and approximately 2 standard deviation resolution in the relativistic rise region. Outside the central tracking chambers are plastic scintillation counters that are used as fast elements in the trigger system and also provide particle identification information from time-of-flight measurements. Beyond the time-of-flight system is the electromagnetic calorimeter, consisting

of 7800 thallium-doped cesium iodide crystals. The central “barrel” region of the calorimeter covers about 75% of the solid angle and has an energy resolution of about 4% at 100 MeV and 1.2% at 5 GeV. Two endcap regions of the crystal calorimeter extend solid angle coverage to about 98% of 4π , although with somewhat worse energy resolution than the barrel region. The tracking system, time-of-flight counters, and calorimeter are all contained within a 1.5 T superconducting coil.

To suppress $\tau\tau$, $\gamma\gamma$, low-multiplicity QED, and other backgrounds while maintaining relatively high $q\bar{q}$ event reconstruction efficiency, the following requirements are imposed to define our hadronic event sample:

1. At least 5 detected, good quality, charged tracks ($N_{\text{chrg}} \geq 5$).
2. The total visible energy E_{vis} ($=E_{\text{chrg}} + E_{\text{neutral}}$) should be greater than the single beam energy: $E_{\text{vis}} > E_{\text{beam}}$.
3. The z-component of the missing momentum must satisfy: $\frac{|p_z^{\text{miss}}|}{E_{\text{vis}}} < 0.3$.
4. To suppress events originating as collisions of e^\pm beam particles with gas or the vacuum chamber walls, we require that the reconstructed event vertex (defined as z_{vrtx}) be within 5.5 cm in z (\hat{z} defined above as the e^+ beam direction) and 2 cm in cylindrical radius of the nominal interaction point.
5. In addition to these primary requirements, additional criteria are imposed to remove backgrounds remaining at the $\sim 1\%$ level, as well as to suppress events with hard initial state radiation, for which theoretical uncertainties are large. These are:
 - (a) No more than two identified electrons are in the event.
 - (b) The ratio R_2 of the second to the zeroth Fox-Wolfram moments [5] for the event should satisfy $R_2 < 0.9$.
 - (c) The ratio of calorimeter energy contained in showers that match to charged particles relative to the scalar sum of the momenta of all the charged particles in the drift chamber ($\frac{E}{p}$) must be less than 0.9.
 - (d) The most energetic photon candidate detected in the event must have a measured energy less than 0.75 of the beam energy ($x_\gamma \equiv \frac{E_\gamma^{\text{max}}}{E_{\text{beam}}} < 0.75$). This requirement reduces the uncertainty from radiative corrections.

Figures 1–7 show comparisons between our candidate hadronic event sample in data and the Monte Carlo sample (arrows indicate our cut values). Simulated hadronic events are produced using the JETSET 7.3 $q\bar{q}$ event generator [6] run through a full GEANT-based [7] detector simulation. Tau-pair events use the KORALB [8] event generator in conjunction with the same detector simulation. In all of these comparison plots, both the data and the ‘Monte Carlo sum’ have been normalized to unit area in the ‘good’ acceptance region. We also use this Monte Carlo event sample to determine the efficiency for $q\bar{q}$ events to pass our hadronic event selection requirements. We note that, according to the Monte Carlo simulation, the trigger inefficiency with the default event selection criteria is less than 0.1%. This has been checked with the data by counting how many hadronic events triggered only a minimum bias, pre-scaled trigger line.

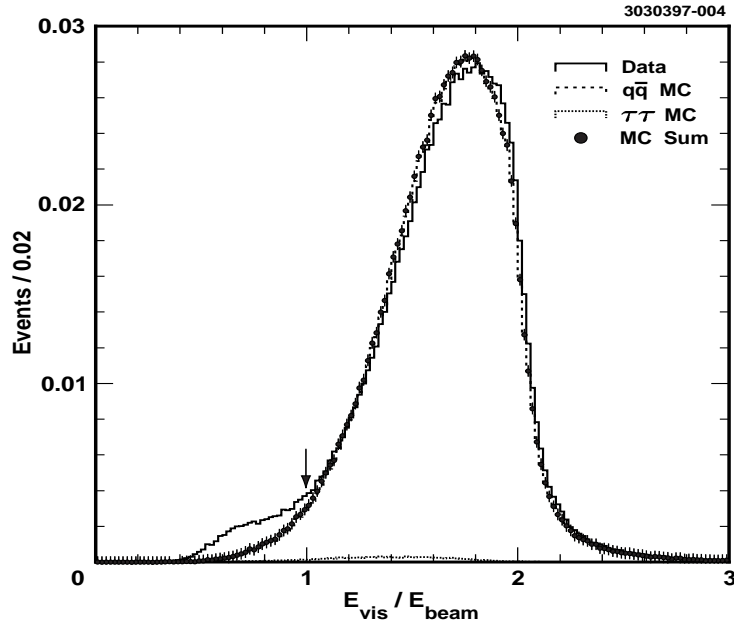


FIG. 1. Normalized visible energy distribution for data (solid), $q\bar{q}$ Monte Carlo (dashed), and $\tau\tau$ Monte Carlo (dotted). Sum of $q\bar{q}$ plus $\tau\tau$ Monte Carlo is shown as crosses.

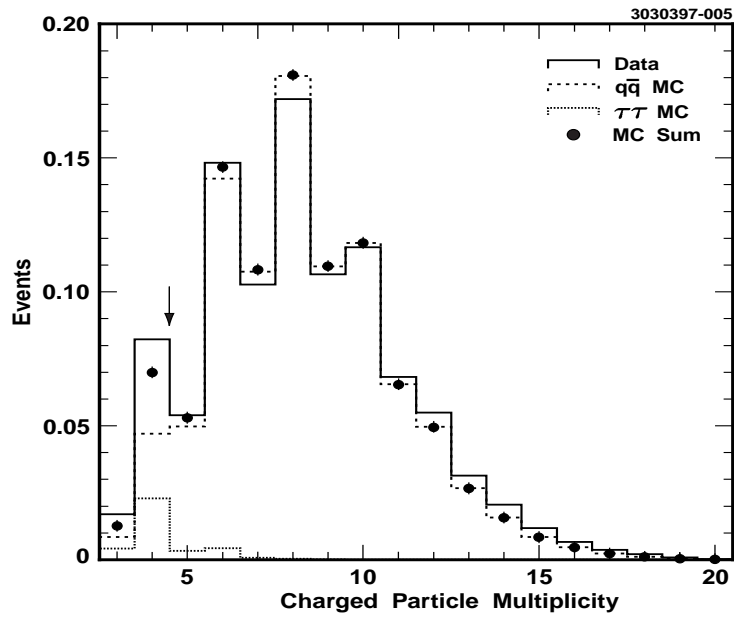


FIG. 2. Normalized charged multiplicity distribution for data vs. Monte Carlo.

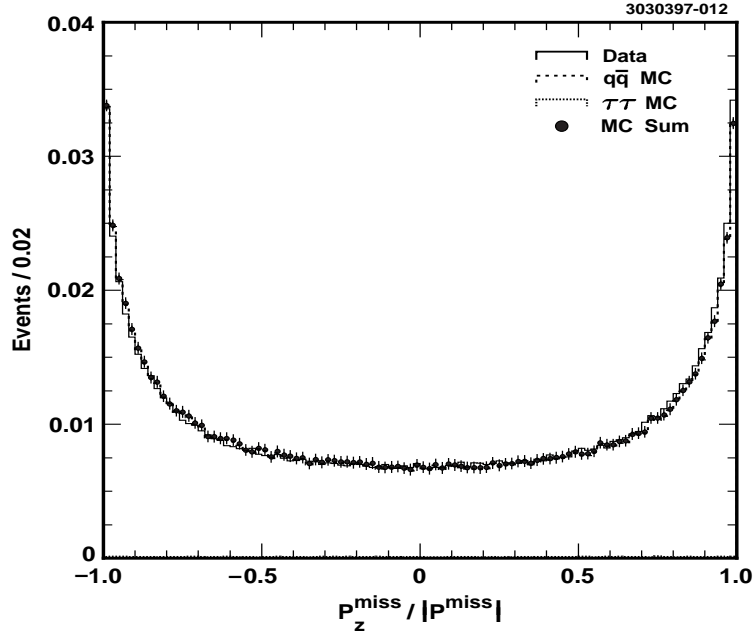


FIG. 3. Distribution of z-component (i.e., direction cosine) of missing momentum $P_z^{miss}/|P^{miss}|$ for data vs. Monte Carlo (this variable is not cut on).

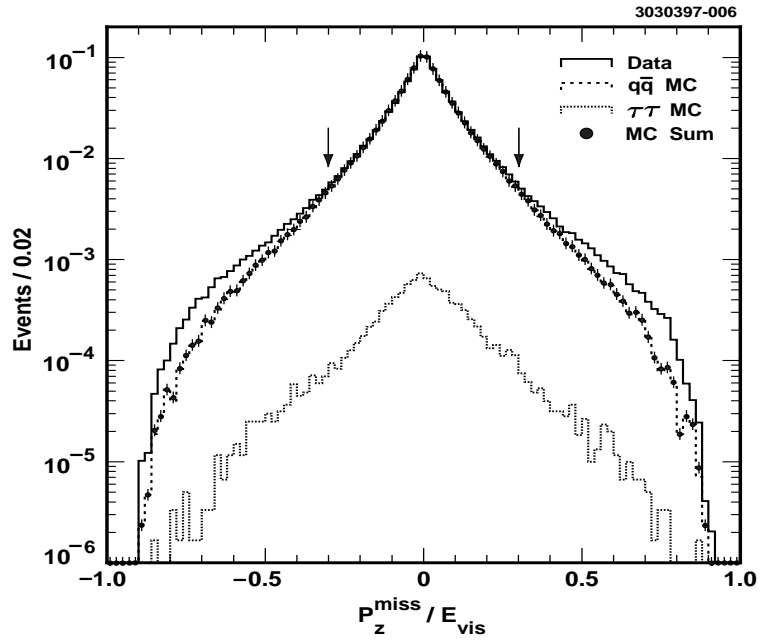


FIG. 4. Ratio of $P_z^{miss}/E_{visible}$ for data vs. Monte Carlo. Two-photon collisions, and beam-gas interactions tend to populate the regions away from zero and towards ± 1 in this plot.

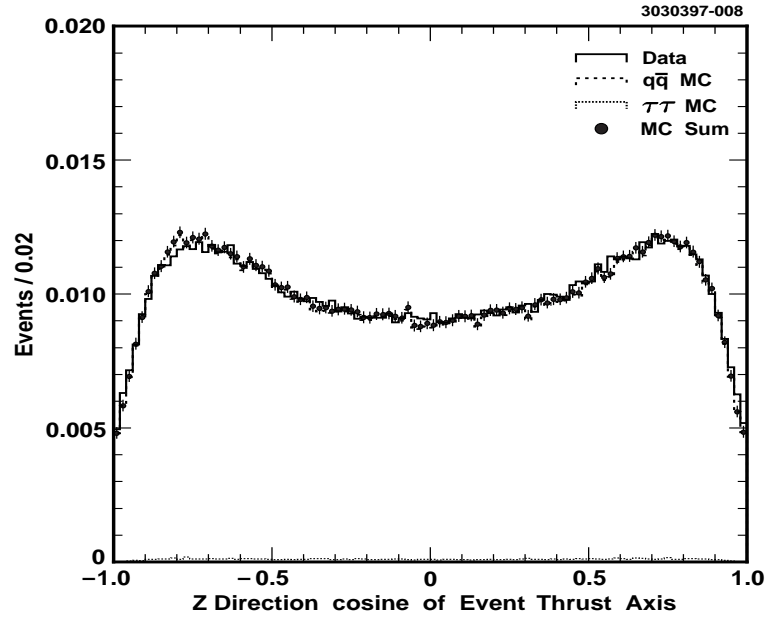


FIG. 5. Z-component of thrust axis for data vs. Monte Carlo (this variable is not cut on).

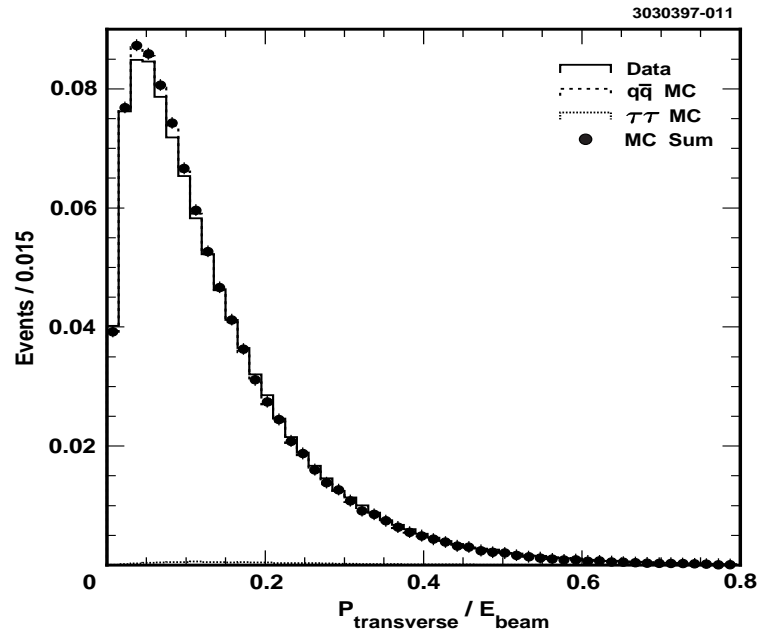


FIG. 6. Ratio of transverse momentum relative to visible energy (this variable is not cut on).

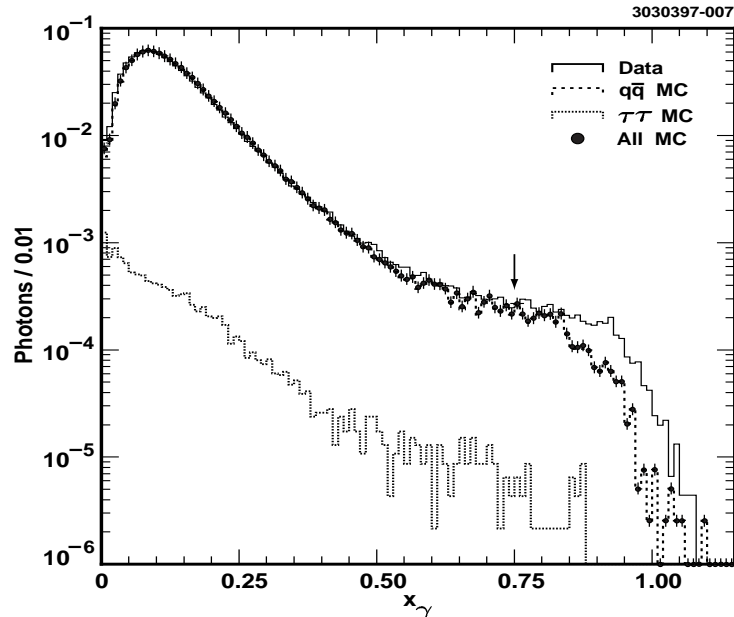


FIG. 7. Comparison of data vs. Monte Carlo spectrum of most energetic photon observed in event.

III. BACKGROUNDS

After imposition of the above event selection criteria, we are left with a sample of 4.00×10^6 candidate hadronic events. Small backgrounds still remain. These are enumerated as follows:

1. Backgrounds from $e^+e^- \rightarrow \tau^+\tau^-(\gamma)$ events are subtracted statistically using a large Monte Carlo sample of KORALB tau-pair events. These events comprise $(1.3 \pm 0.1)\%$ (statistical error only) of the sample passing the above event selection criteria.
2. Backgrounds from the narrow Υ resonances can be explicitly determined from data using $e^+e^- \rightarrow \gamma\Upsilon(3S/2S)$; $\Upsilon(3S/2S) \rightarrow \pi^+\pi^-\Upsilon(1S)$; $\Upsilon(1S) \rightarrow l^+l^-$ events. These events are distinctive by their characteristic topology of two low-momentum pions accompanied by two very high momentum, back-to-back leptons; the photon generally escapes undetected along the beam axis. As shown in Figure 8, we observe these events as distinct peaks in the mass distribution recoiling against two low-momentum pions in events also containing two high-energy muons. (The recoil mass is calculated from: $M_{recoil} = \sqrt{(2E_{beam} - E_{\pi_1} - E_{\pi_2})^2 - (\vec{p}_{\pi_1} + \vec{p}_{\pi_2})^2}$, and therefore neglects the four-momentum of the initial state radiation photon.) Backgrounds from QED processes ($e^+e^- \rightarrow \gamma l^+l^-$; $\gamma \rightarrow e^+e^-$) can be suppressed by requiring that the candidate dipion system not be colinear with either of the final state leptons. Knowing the branching fractions [9] for $\Upsilon(2S) \rightarrow \pi\pi\Upsilon(1S)$ ($18.5 \pm 0.8\%$) and $\Upsilon(3S) \rightarrow \pi\pi\Upsilon(1S)$ ($4.5 \pm 0.2\%$), the leptonic branching fraction for the $\Upsilon(1S)$ ($2.5 \pm 0.1\%$), and the reconstruction efficiency for such events (~ 0.7), we can determine the contribution to the observed hadronic cross-section from the $\Upsilon(2S)$ and $\Upsilon(3S)$ resonances

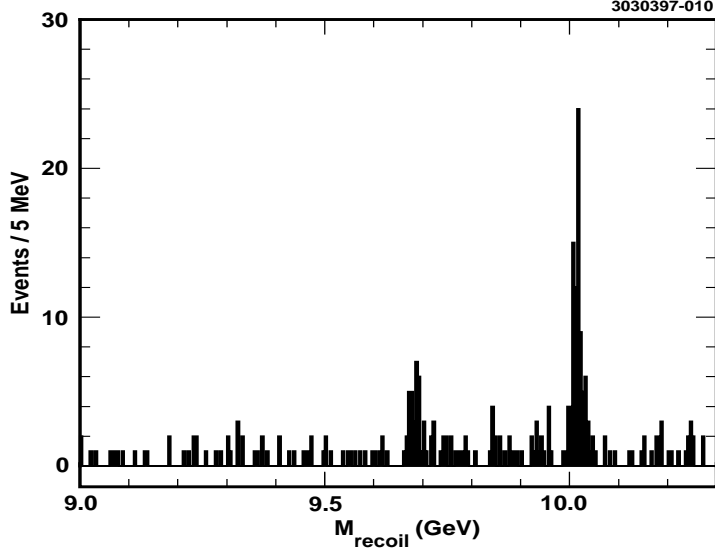


FIG. 8. Mass recoiling against two charged particles, assumed to be pions, in events consistent with the kinematics for: $e^+e^- \rightarrow \gamma\Upsilon(3S/2S)$; $\Upsilon(3S/2S) \rightarrow \Upsilon(1S)\pi^+\pi^-$; $\Upsilon(1S) \rightarrow l^+l^-$. Two peaks are evident; the leftmost peak corresponds to $\Upsilon(3S) \rightarrow \pi^+\pi^-\Upsilon(1S)$ transitions, the rightmost peak corresponds to $\Upsilon(2S) \rightarrow \pi^+\pi^-\Upsilon(1S)$ transitions. The calculated recoil mass differs from the true $\Upsilon(1S)$ mass due to our neglecting the (undetected) radiated photon in the recoil mass calculation.

directly, by simply measuring the event yields in the peaks shown in Figure 8, and correcting by branching fractions and efficiency.

For the contribution from the $\Upsilon(1S)$ resonance, we proceed by assuming that the photon spectrum varies as: $\frac{dN}{dE_\gamma} \sim \frac{1}{E_\gamma}$, and that the production of a given Upsilon resonance is proportional to its dielectron width Γ_{ee} . This gives a fairly simple prediction for the ratios expected for a given Upsilon resonance, since $E_\gamma \sim (10.52 - M_\Upsilon)$ GeV. We would expect that the production cross-section for $\Upsilon\gamma$ in e^+e^- annihilation therefore varies as: $\Gamma(e^+e^- \rightarrow \Upsilon\gamma) \propto \frac{\Gamma_{ee}^\Upsilon}{E_\gamma}$. This allows us to infer an expected production cross-section for $\gamma\Upsilon(1S)$ based on our measurements for $\gamma\Upsilon(2S)$ and $\gamma\Upsilon(3S)$ production. We compare our extrapolated cross-section for $e^+e^- \rightarrow \gamma\Upsilon(1S)$ through this procedure with theory in order to estimate the magnitude of this correction. Combining our data with the theoretical predictions of Teubner et al. [2], we determine that the $\gamma\Upsilon(1S)$, $\gamma\Upsilon(2S)$, and $\gamma\Upsilon(3S)$ events comprise $(1.8 \pm 0.6)\%$ of the observed hadronic cross-section, where the error includes the uncertainties in the Upsilon decay branching fractions and detection efficiencies as well as the deviations between the theoretical and measured values.

3. Two-photon collisions, which produce hadrons in the final state via $e^+e^- \rightarrow e^+e^-\gamma\gamma \rightarrow e^+e^- + \text{hadrons}$, are determined by running final-state specific $\gamma\gamma$ collision Monte Carlo events, and also by determining the magnitude of possible excesses in the E_{visible} vs. $P_{\text{transverse}}$ plane for data over $q\bar{q}$ Monte Carlo. These are determined to comprise $(0.8 \pm 0.4)\%$ of our total hadronic event sample.

4. Beam-wall, beam-gas, and cosmic ray events are expected to have a flat event vertex distribution in the interval $|z_{vrtx}| < 10$ cm; such events are subtracted using a sample having a vertex in the interval $5.5\text{cm} < |z_{vrtx}| < 10\text{cm}$, and extrapolating into the ‘good’ acceptance region ($|z_{vrtx}| < 5.5$ cm). These backgrounds are determined to comprise $\sim (0.2 \pm 0.1)\%$ of our hadronic sample.
5. Remaining QED backgrounds producing 2 or more electrons or muons in the final state are assessed using a high-statistics sample of Monte Carlo events (to 3^{rd} order in α_{QED}), and found to be $\leq 0.1\%$ of the sample passing the above hadronic event selection requirements.

Summing these estimates results in a net background fraction $f = (4.1 \pm 0.7)\%$. We note that, as this error is assessed partly by examining the difference between Monte Carlo hadronic event simulations and our data, this error also includes Monte Carlo modeling errors.

IV. EFFICIENCIES AND RADIATIVE CORRECTIONS

The computation of R is performed with

$$R = \frac{N_{had}(1 - f)}{\mathcal{L}\epsilon_{had}(1 + \delta)\sigma_{\mu\mu}^0}, \quad (2)$$

where N_{had} is the number of events classified as hadronic, f is the fraction of selected events attributable to all background processes, ϵ_{had} is the efficiency for triggering and selection of events, δ is the fractional increase in hadronic cross section due to electromagnetic radiative corrections to that cross section, $\sigma_{\mu\mu}^0$ is the point cross section for muon pair production ($86.86\text{nb}/E_{cm}^2(\text{GeV}^2)$), and \mathcal{L} is the measured integrated luminosity. The luminosity is determined from wide angle e^+e^- , $\gamma\gamma$, and $\mu^+\mu^-$ final states and is known to $\pm 1\%$ [3]. For the data analyzed here, the integrated luminosity \mathcal{L} is equal to (1.521 ± 0.015) fb $^{-1}$.

To calculate R , we must therefore evaluate Eqn. 2. If the initial state radiation corrections were known precisely, we would be able to calculate the denominator term $\epsilon(1 + \delta)$ with very good precision. However, since the uncertainties become very large as the center-of-mass energy approaches $c\bar{c}$ threshold ($\sqrt{s} \sim 4$ GeV), the preferred procedure is to choose some explicit cut-off in initial state radiation (ISR) photon energy that makes us as insensitive as possible to the corrections in this high ISR photon energy/low hadronic recoil mass region. We therefore purposely design our selection criteria so that our efficiency for events with highly energetic ISR photons approaches zero. By choosing cuts that drive ϵ to zero beyond some kinematic point, we ensure that the product $\epsilon \times (1 + \delta)$ is insensitive to whatever value of δ may be prescribed by theory beyond our cut. Thus, although there is a large uncertainty in the magnitude of the initial state radiation correction for large values of radiated photon momentum, we have minimized our sensitivity to this theoretical uncertainty. Figure 9 displays our efficiency for an $e^+e^- \rightarrow \gamma q\bar{q}$ event to pass our hadronic event criteria as a function of the scaled photon energy $x_\gamma \equiv \frac{E_\gamma}{E_{beam}}$. We note that for $x_\gamma > 0.75$ (corresponding to a $q\bar{q}$ recoil mass of $M_{recoil} < 5.25 \text{ GeV}/c^2$), our integrated event-finding efficiency $\epsilon_{had} < 1\%$. For $x_\gamma > 0.75$, we have therefore minimized our sensitivity to modeling uncertainties in this kinematic regime – increasing the initial state radiation contribution to this region results in a compensating loss of overall efficiency such that the product of $\epsilon(1 + \delta)$ remains relatively constant. For our event selection criteria, we thus select the value of $\epsilon(1 + \delta)(x_\gamma^{max} = 0.75) = 0.90 \pm 0.01$, where the error reflects the systematic uncertainty in the radiative corrections.

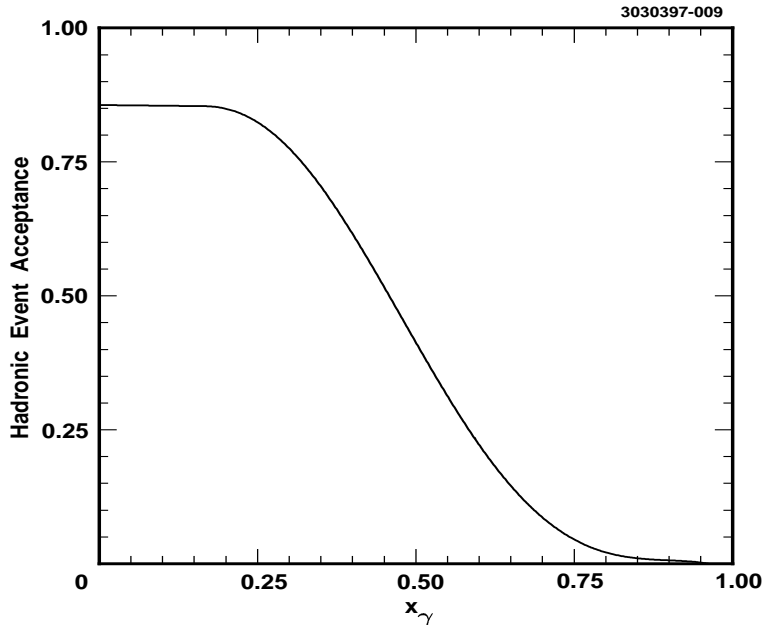


FIG. 9. Efficiency for reconstructing $e^+e^- \rightarrow \gamma q\bar{q}$ event, as a function of the scaled photon momentum $x_\gamma \equiv E_\gamma/E_{beam}$.

After subtracting all backgrounds, dividing by the total luminosity, and normalizing to the mu-pair point cross-section, we obtain a value of $R = 3.56 \pm 0.01$ (statistical error only).

V. SYSTEMATIC ERRORS AND CONSISTENCY CHECKS

We have checked our results in several ways. Backgrounds can be suppressed significantly by tightening the minimum charged track multiplicity to $N_{chrg} \geq 7$, albeit at a loss of $\sim 20\%$ in the overall event-reconstruction efficiency. Imposition of such a cut leads to only a -0.4% change in the calculated value of R . Continuum data have been collected over 17 distinct periods from 1990-1996, covering many different trigger configurations and running conditions. We find a 0.3% rms variation between the various datasets used (the statistical error on R within each dataset is of order 0.1%). We can check contributions due to the narrow Upsilon resonances by calculating R using a small amount ($5pb^{-1}$) of continuum data taken just below the $\Upsilon(2S)$ resonance, at $E_{beam}=4.995$ GeV. We find that the value of R calculated using the $\Upsilon(2S)$ continuum agrees with that calculated using the $\Upsilon(4S)$ continuum to within one statistical error ($1\sigma_{stat}$). Systematic errors are summarized in Table I.

Systematic error summary

Source	Error
$\epsilon \times (1 + \delta)$	1%
\mathcal{L}	1%
Background Uncertainty/Hadronic Event Modeling Uncertainty	0.7%
Dataset-to-dataset variation	0.3%
Total	1.8%

TABLE I. Systematic errors in R analysis.

VI. EXTRACTION OF α_s

Using the expansion for R in powers of α_s/π given previously, with coefficients appropriate for this center of mass energy [2], we can evaluate the strong coupling constant. Using that expression, our value for R translates to $\alpha_s(10.52 \text{ GeV}) = 0.20 \pm 0.01 \pm 0.06$.

The strong coupling constant α_s can be written as a function of the basic QCD parameter $\Lambda_{\overline{MS}}$, defined in the modified minimal subtraction scheme [9],

$$\alpha_s(\mu) = \frac{4\pi}{b_0 x} \left(1 - \frac{2b_1 \ln(x)}{b_0^2 x} + \frac{4b_1^2}{b_0^4 x^2} \times \left([\ln(x) - \frac{1}{2}]^2 + \frac{b_2 b_0}{8b_1^2} - \frac{5}{4} \right) \right) \quad (3)$$

where $b_0 = (11 - 2n_f/3)$, μ is the energy scale, in GeV, at which α_s is being evaluated, $b_1 = \frac{51 - 19n_f}{3}$, $b_2 = 2857 - \frac{5033n_f}{9} + \frac{325n_f^2}{27}$, $x = \ln(\mu^2/\Lambda_{\overline{MS}}^2)$, and n_f is the number of light quark flavors which participate in the process. To determine the value of $\alpha_s(90 \text{ GeV})$ implied by our measurement, we must evolve α_s across the discontinuity in $\Lambda_{\overline{MS}}$ when the five-flavor threshold is crossed from the four-flavor regime. We do so using the next-to-next-to leading order (NNLO) prescription, as described in [9]: a) We substitute $\alpha_s(10.52)$ into Eqn. (3) to determine a value for $\Lambda_{\overline{MS}}$ in the four-flavor continuum (obtaining $\Lambda_{\overline{MS}}(udcs) = 498 \text{ MeV}$). b) With that value of $\Lambda_{\overline{MS}}$, we can now again use Eqn. (3) to determine the value of α_s at the five-flavor threshold when the b -quark pole mass (we use $m_{b,pole} = 4.7 \text{ GeV}$) is crossed, and then use that value of α_s , as well as $n_f = 5$ in Eqn. (3) to determine $\Lambda_{\overline{MS}}$ appropriate for the five-flavor continuum. c) Assuming that this value of $\Lambda_{\overline{MS}}$ is constant in the entire five-flavor energy region, we can now evolve α_s up to the Z -pole, to obtain $\alpha_s(M_Z) = 0.13 \pm 0.005 \pm 0.03$, in good agreement with the world average $\alpha_s(M_Z) = 0.118 \pm 0.003$ [9].

VII. SUMMARY

Near $\sqrt{s} = 10 \text{ GeV}$, R has been measured by many experiments, as shown in Table II. The measurement of R described here is the most precise below the Z^0 . Theoretical uncertainties in QED radiative corrections (in the acceptance $(\epsilon \times (1 + \delta))$ and luminosity [3]) contribute about the same amount to the systematic error as do backgrounds and efficiencies. Substantially improving this measurement will require progress on radiative corrections as well as on experimental techniques. Our R value is in good agreement with the previous world average, including a recent determination by the MD-1 Collaboration [18]. Our implied value of α_s is in agreement with higher energy determinations of this quantity.

Experiment	$\sqrt{s}(\text{GeV})$	R
PLUTO [10]	9.4	$3.67 \pm 0.23 \pm 0.29$
DASPII [11]	9.4	$3.37 \pm 0.16 \pm 0.28$
DESY-Heidelberg [12]	9.4	$3.80 \pm 0.27 \pm 0.42$
LENA [13]	9.1-9.4	$3.34 \pm 0.09 \pm 0.18$
LENA [13]	7.4-9.4	$3.37 \pm 0.06 \pm 0.23$
CUSB [14]	10.5	$3.54 \pm 0.05 \pm 0.40$
CLEO 83 [15]	10.5	$3.77 \pm 0.06 \pm 0.24$
Crystal Ball [16]	9.4	$3.48 \pm 0.04 \pm 0.16$
ARGUS [17]	9.36	$3.46 \pm 0.03 \pm 0.13$
MD-1 [18]	7.25-10.34	$3.58 \pm 0.02 \pm 0.14$
Previous Expts., Weighted Average	≈ 9.5	3.58 ± 0.07
CLEO 97 (this work)	10.5	$3.56 \pm 0.01 \pm 0.07$

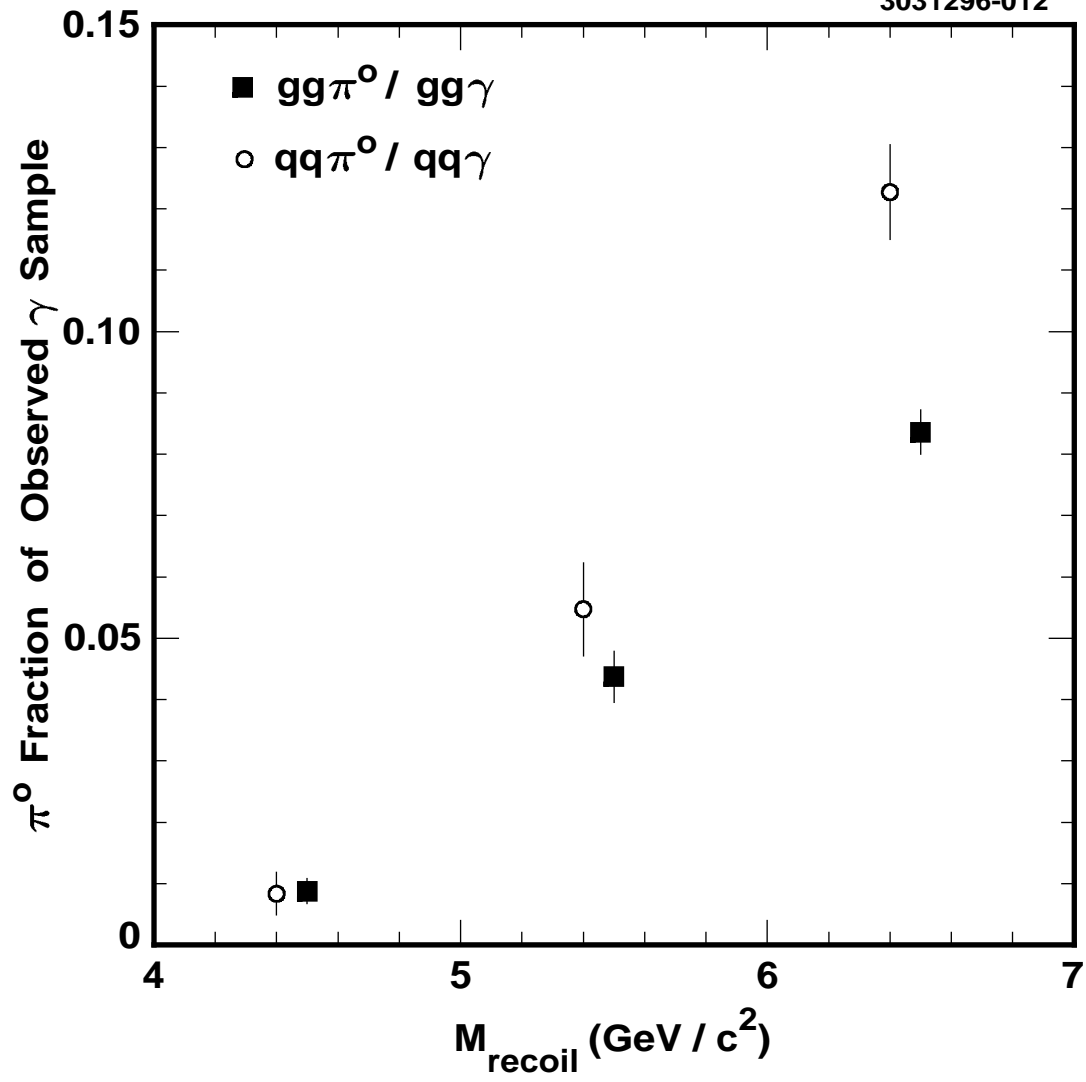
TABLE II. Summary of inclusive cross section measurements.

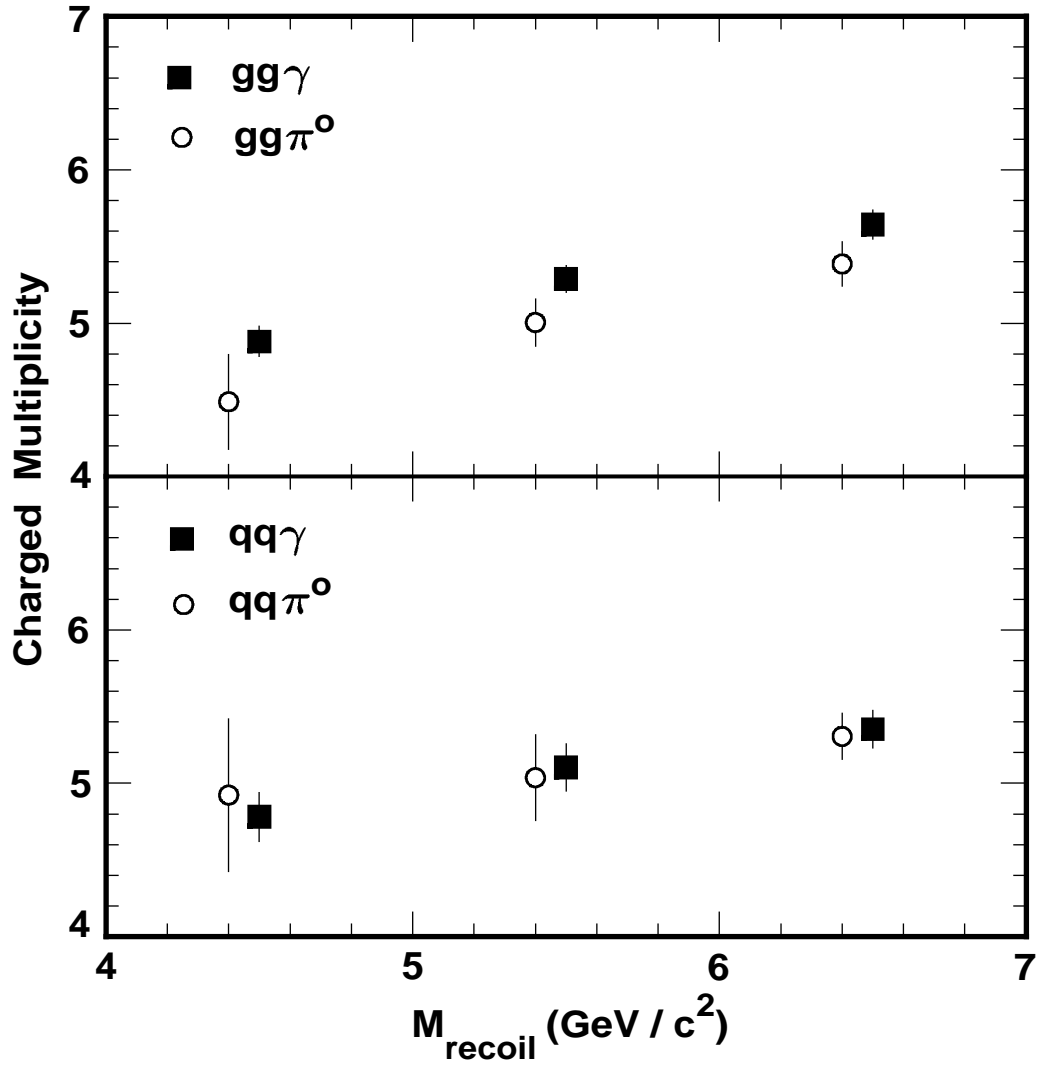
VIII. ACKNOWLEDGMENTS

We gratefully acknowledge the effort of the CESR staff in providing us with excellent luminosity and running conditions. J.P.A., J.R.P., and I.P.J.S. thank the NYI program of the NSF, M.S. thanks the PFF program of the NSF, G.E. thanks the Heisenberg Foundation, K.K.G., M.S., H.N.N., T.S., and H.Y. thank the OJI program of DOE, J.R.P., K.H., M.S. and V.S. thank the A.P. Sloan Foundation, R.W. thanks the Alexander von Humboldt Stiftung, and M.S. thanks Research Corporation for support. This work was supported by the National Science Foundation, the U.S. Department of Energy, and the Natural Sciences and Engineering Research Council of Canada.

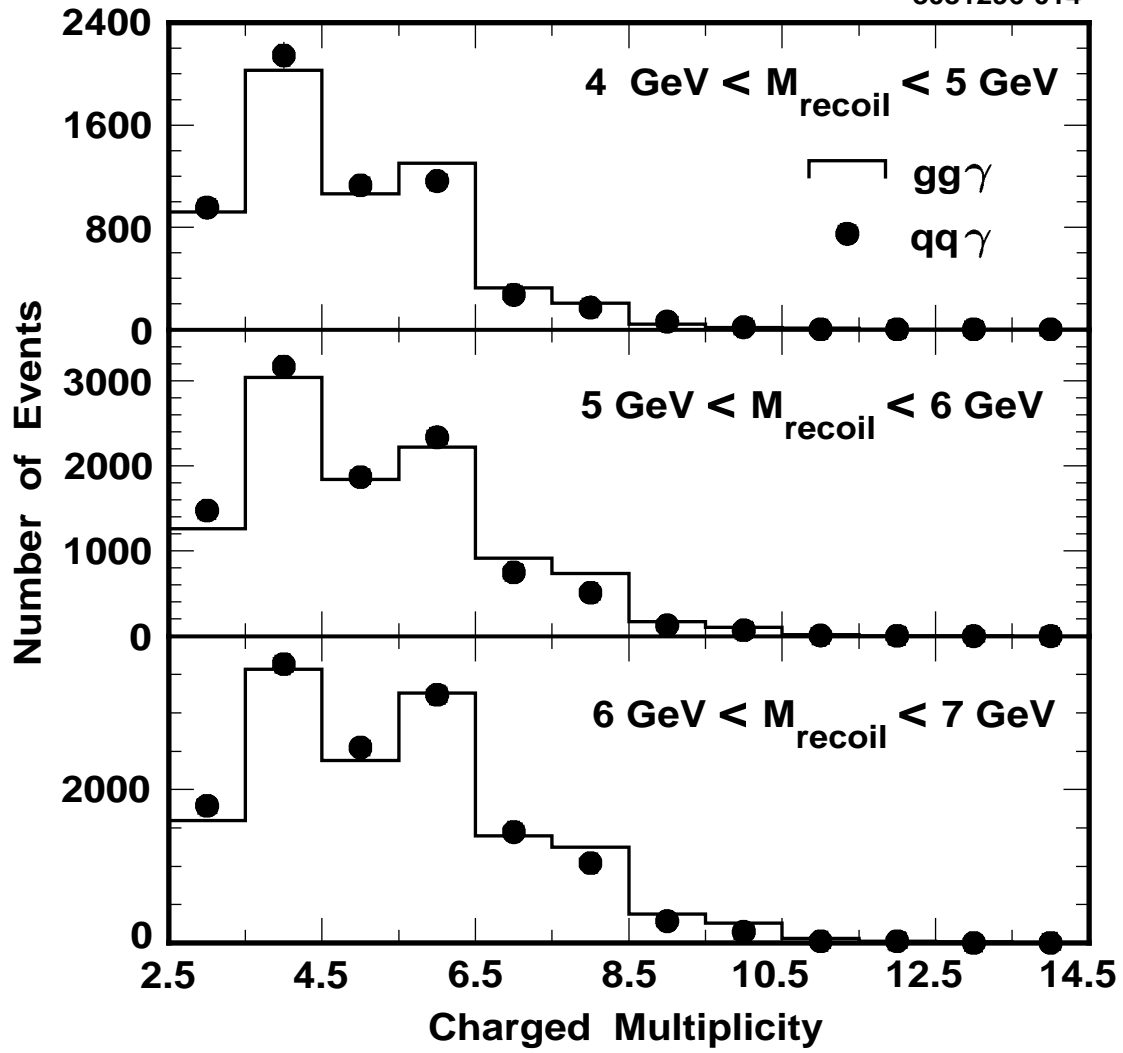
REFERENCES

- [1] S. G. Gorishny, A. L. Kataev, S. A. Larin, Phys. Lett. **B259**, 144 (1991); L. R. Surguladze and M. A. Samuel, Phys. Rev. Lett. **66**, 560 (1991), and K. G. Chetyrkin, Preprint hep-ph/9608480.
- [2] K. G. Chetyrkin, J. H. Kühn, and T. Teubner, Preprint TTP 96-35, DTP/96/80, hep-ph/9609411; K. G. Chetyrkin and J. H. Kühn, Phys. Lett. **B342**, 356 (1995); K. G. Chetyrkin and J. H. Kühn, Phys. Lett. **B308**, 127 (1993).
- [3] CLEO Collaboration, G. Crawford *et al.*, Nucl. Instrum. Methods Phys. Res., Sect. A **345**, 429 (1994).
- [4] CLEO Collab., Y. Kubota *et al.*, Nucl. Instr. Meth. **A320**, 66 (1992).
- [5] G. C. Fox and S. Wolfram, Phys. Rev. Lett. **41**, 1581 (1978), and G. C. Fox and S. Wolfram, Phys. Lett. **B82**, 134 (1979).
- [6] S. J. Sjostrand, LUND 7.3, CERN-TH-6488-92 (1992).
- [7] R. Brun *et al.*, GEANT v. 3.14, CERN Report No. CERN CC/EE/84-1 (1987).
- [8] We use KORALB (v.2.2) / TAUOLA (v.2.4). References for earlier versions are: S. Jadach and Z. Was, Comput. Phys. Commun. **36**, 191 (1985); **64**, 267 (1991); S. Jadach, J. H. Kühn, and Z. Was, Comput. Phys. Commun. **64**, 275 (1991); **70**, 69 (1992); **76**, 361 (1993).
- [9] Particle Data Group, R.M. Barnett, *et al.*, Phys. Rev. **D54**, (1996).
- [10] The PLUTO Collaboration, L. Criegee *et al.*, Phys. Rep. C83 (1982), 151
- [11] The DASP-II Collaboration, H. Albrecht *et al.*, Phys. Lett. 116B (1982) 383
- [12] P. Bock *et al.*, Z. Phys. C 6 (1980) 125.
- [13] The LENA Collaboration, B. Niczporuck *et al.*, Z. Phys. C 15, 299 (1982).
- [14] The CUSB Collaboration, E. Rice *et al.*, Phys. Rev. Lett. 48, 906 (1982).
- [15] The CLEO Collaboration, R. Giles *et al.*, Phys. Rev. D29, 1285 (1984).
- [16] The Crystal Ball Collaboration, Z. Jakubowski *et al.*, Z. Phys. C 40, 49 (1988).
- [17] The ARGUS Collaboration, H. Albrecht *et al.*, Z. Phys. C 53, 13 (1991).
- [18] The MD-1 Collaboration, A.E. Blinov *et al.*, Z.Phys. C 70, 31 (1996).





3031296-014



3031296-015

